

Dinitrosyl Iron Complexes (DNICs): From Biomimetic Synthesis and Spectroscopic Characterization toward Unveiling the Biological and Catalytic Roles of DNICs

Published as part of the Accounts of Chemical Research special issue "Synthesis in Biological Inorganic Chemistry".

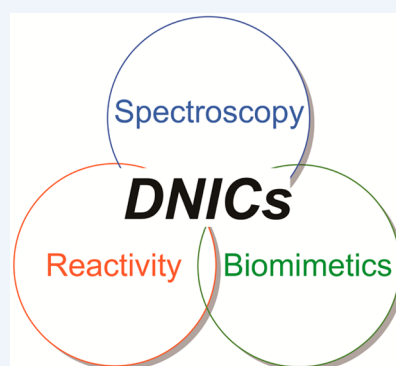
Ming-Li Tsai, Chih-Chin Tsou, and Wen-Feng Liaw*

Department of Chemistry and Frontier Research Center on Fundamental and Applied Sciences of Matters, National Tsing Hua University, Hsinchu 30013, Taiwan

CONSPECTUS: Dinitrosyl iron complexes (DNICs) have been recognized as storage and transport agents of nitric oxide capable of selectively modifying crucial biological targets via its distinct redox forms (NO^+ , NO^\bullet and NO^-) to initiate the signaling transduction pathways associated with versatile physiological and pathological responses. For decades, the molecular geometry and spectroscopic identification of $\{\text{Fe}(\text{NO})_2\}^n$ DNICs ($\{\text{Fe}(\text{NO})_x\}^n$ where n is the sum of electrons in the Fe 3d orbitals and NO π^* orbitals based on Enemark–Feltham notation) in biology were limited to tetrahedral ($\text{CN} = 4$) and EPR g -value ~ 2.03 , respectively, due to the inadequacy of structurally well-defined biomimetic DNICs as well as the corresponding spectroscopic library accessible in biological environments.

The developed synthetic methodologies expand the scope of DNICs into nonclassical square pyramidal and trigonal bipyramidal ($\text{CN} = 5$) and octahedral ($\text{CN} = 6$) $\{\text{Fe}(\text{NO})_2\}^n$ DNICs, as well as two/three accessible redox couples for mononuclear $\{\text{Fe}(\text{NO})_2\}^{9/10}$ and dinuclear $[\{\text{Fe}(\text{NO})_2\}^{9/10}-\{\text{Fe}(\text{NO})_2\}^{9/10}]$ DNICs with biologically relevant S/O/N ligation modes. The unprecedented molecular geometries and electronic states of structurally well-defined DNIC models provide the foundation to construct a spectroscopic library for uncovering the identity of DNICs in biological environments as well as to determine the electronic structures of the $\{\text{Fe}(\text{NO})_2\}$ core in qualitative and quantitative fashions by a wide range of spectroscopic methods. On the basis of ^{15}N NMR, electron paramagnetic resonance (EPR), IR, cyclic voltammetry (CV), superconducting quantum interference device (SQUID) magnetometry, UV–vis, single-crystal X-ray crystallography, and Fe/S K-edge X-ray absorption and Fe $K\beta$ X-ray emission spectroscopies, the molecular geometry, ligation modes, nuclearity, and electronic states of the mononuclear $\{\text{Fe}(\text{NO})_2\}^{9/10}$ and dinuclear $[\{\text{Fe}(\text{NO})_2\}^{9/10}-\{\text{Fe}(\text{NO})_2\}^{9/10}]$ DNICs could be characterized and differentiated. In addition, Fe/S K-edge X-ray absorption spectroscopy of tetrahedral DNICs deduced the qualitative assignment of Fe/NO oxidation states of $\{\text{Fe}(\text{NO})_2\}^n$ DNICs as a resonance hybrid of $\{\text{Fe}^{\text{II}}(\bullet\text{NO})(\text{NO}^-)\}^n$ and $\{\text{Fe}^{\text{III}}(\text{NO}^-)_2\}^n$ electronic states; the quantitative NO oxidation states of $[(\text{PhS})_3\text{Fe}(\text{NO})]^-$, $[(\text{PhS})_2\text{Fe}(\text{NO})_2]^-$, and $[(\text{PhO})_2\text{Fe}(\text{NO})_2]^-$ were further achieved by newly developed valence to core Fe $K\beta$ X-ray emission spectroscopy as -0.58 ± 0.18 , -0.77 ± 0.18 , and -0.95 ± 0.18 , respectively.

The in-depth elaborations of electronic structures provide credible guidance to elucidate (a) the essential roles of DNICs modeling the degradation and repair of $[\text{Fe}-\text{S}]$ clusters under the presence of NO, (b) transformation of DNIC into S-nitrosothiol (RSNO)/N-nitrosamine (R_2NNO) and $\text{NO}^+/\text{NO}^\bullet/\text{NO}^-$, (c) nitrite/nitrate activation producing NO regulated by redox shuttling of $\{\text{Fe}(\text{NO})_2\}^n$ and $\{\text{Fe}(\text{NO})_2\}^{10}$ DNICs, and (d) DNICs as H_2S storage and cellular permeation pathway of DNIC/Roussin's red ester (RRE) for subsequent protein S-nitrosylation. The consolidated efforts on biomimetic synthesis, inorganic spectroscopy, chemical reactivity, and biological functions open avenues to the future designs of DNICs serving as stable inorganic $\text{NO}^+/\text{NO}^\bullet/\text{NO}^-$ donors for pharmaceutical applications.



■ INTRODUCTION

Under physiological control, NO plays versatile roles in important biological functions. In physiological conditions, nitric oxide acts as the endothelium-derived relaxation factor for smooth muscle relaxation, the secondary messenger for signal transduction pathways and the activator or inhibitor for metalloenzymes.¹ In pathological conditions, nitric oxide serves as the precursor for the formation of reactive oxygen and

nitrogen species (OONO^\bullet , OH^\bullet , NO_2^\bullet , etc.) to defend against the invasion of foreign pathogens.¹

The diverse physiological and pathological functions mediated by nitric oxide originate from its intriguing physical and chemical properties. Nitric oxide readily switches among three accessible redox levels NO^+ , NO^\bullet , and NO^- , and each of

Received: December 23, 2014

Published: April 2, 2015

the redox states possesses unique chemical reactivity toward biological targets. Specifically, NO^+ may primarily exert post-translational modifications of S-nitrosylating cysteine residues. The formation of $\text{S}_{\text{Cys}}-\text{NO}$ of the NMDA (*N*-methyl-D-aspartate) receptor has been reported to downregulate its activity and result in neuroprotective effects in the central nervous system.² In comparison, NO^\bullet is inert to amino acid residues; however it may bind transition metals. Coordination of NO^\bullet to the ferrous center of soluble guanylate cyclase induces a conformational rearrangement and triggers subsequent signal transduction pathways for smooth muscle relaxation.³ Although NO^- is capable of initiating post-translational modification on cysteine residues and coordinating to transition metals, orthogonal biological functions compared with NO^+ and NO^\bullet have been reported. It is also known that NO^- undergoes an addition reaction with cysteine residues and reductive nitrosylation of ferric proteins to form the corresponding disulfide/sulfinamide and ferrous–nitrosyl complexes, respectively.⁴

To accommodate the short-lived nitric oxide in complex biological systems, nature has evolved two transitory derivatives of NO, RSNO (*S*-nitrosothiol) and DNICs (dinitrosyl iron complexes), in addition to its biologically inert metabolite nitrite ($[\text{NO}_2]^-$), to serve as storage and transport of NO to specific targets.^{5,6} DNICs were first proposed as $[\text{L}_2\text{Fe}(\text{NO})_2]^n$ with a characteristic electron paramagnetic resonance (EPR) signal *g* value of ~ 2.03 from the reaction of Fe^{II} salt, $\text{NO}_{(\text{g})}$, and anionic ligands.^{7,8} Interestingly, nitric oxide-derived cellular adducts with a similar EPR signature have been ubiquitously observed in biology including in the coculture of stimulated macrophage, tumor-target cells, lipopolysaccharide-treated rat aorta in the presence of *N*-acetylcysteine, and the nitrosylation product of $[\text{Fe}-\text{S}]$ clusters.⁵ Despite the prevalence of the characteristic EPR signal ($g \approx 2.03$) in various physiological and pathological events, the chemical reactivity and biological functions of DNICs have not been elucidated at a molecular level due to the lack of biomimetic studies on structurally well-defined DNIC models.

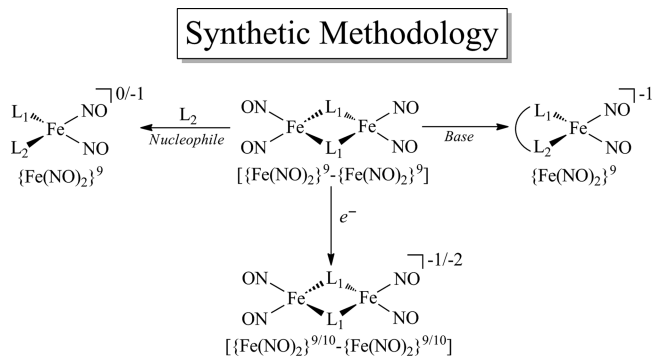
This Account mainly focuses on the recent progress of biomimetic studies on the transformation among classical and nonclassical mononuclear $\{\text{Fe}(\text{NO})_2\}^{9/10}$ and dinuclear $[\{\text{Fe}(\text{NO})_2\}^{9/10}-\{\text{Fe}(\text{NO})_2\}^{9/10}]$ DNICs with biologically relevant S/N/O ligation modes,⁹ the development of a spectroscopic protocol for the identification of DNICs in complex biological systems, and the elucidation of electronic structures of the $[\text{Fe}(\text{NO})_2]$ motif in various DNICs, as well as their contributions to chemical reactivity. Also, the delineated geometry–electronic structure–reactivity relationships provide insights to elaborate the pivotal roles of DNICs in the following fields: (1) the essential roles of DNICs modeling the degradation and repair of $[\text{Fe}-\text{S}]$ clusters under the presence of NO, (2) transformation of DNICs into *S*-nitrosothiol (RSNO)/*N*-nitrosamine (R_2NNO) and $\text{NO}^+/\text{NO}^\bullet/\text{NO}^-$, (3) nitrite/nitrate activation producing NO regulated by redox shuttling of $\{\text{Fe}(\text{NO})_2\}^9$ and $\{\text{Fe}(\text{NO})_2\}^{10}$ DNICs, and (4) DNICs as H_2S storage and the cellular permeation pathway of DNICs and Roussin's red esters (RREs) for subsequent protein S-nitrosylation.

■ SYNTHESIS AND CLASSIFICATION OF DNICs

The biomimetic studies provide a valuable way to unambiguously delineate the correlation between molecular structures and chemical reactivity of DNICs. Three distinct pathways

synthesize mononuclear $\{\text{Fe}(\text{NO})_2\}^{9/10}$ and dinuclear $[\{\text{Fe}(\text{NO})_2\}^{9/10}-\{\text{Fe}(\text{NO})_2\}^{9/10}]$ DNICs were developed to explore the possible binding modes of biologically relevant S-, N-, and O-containing ligands toward the $[\text{Fe}(\text{NO})_2]$ motif and redox states of DNICs (Scheme 1).^{10–24} Three distinct reaction

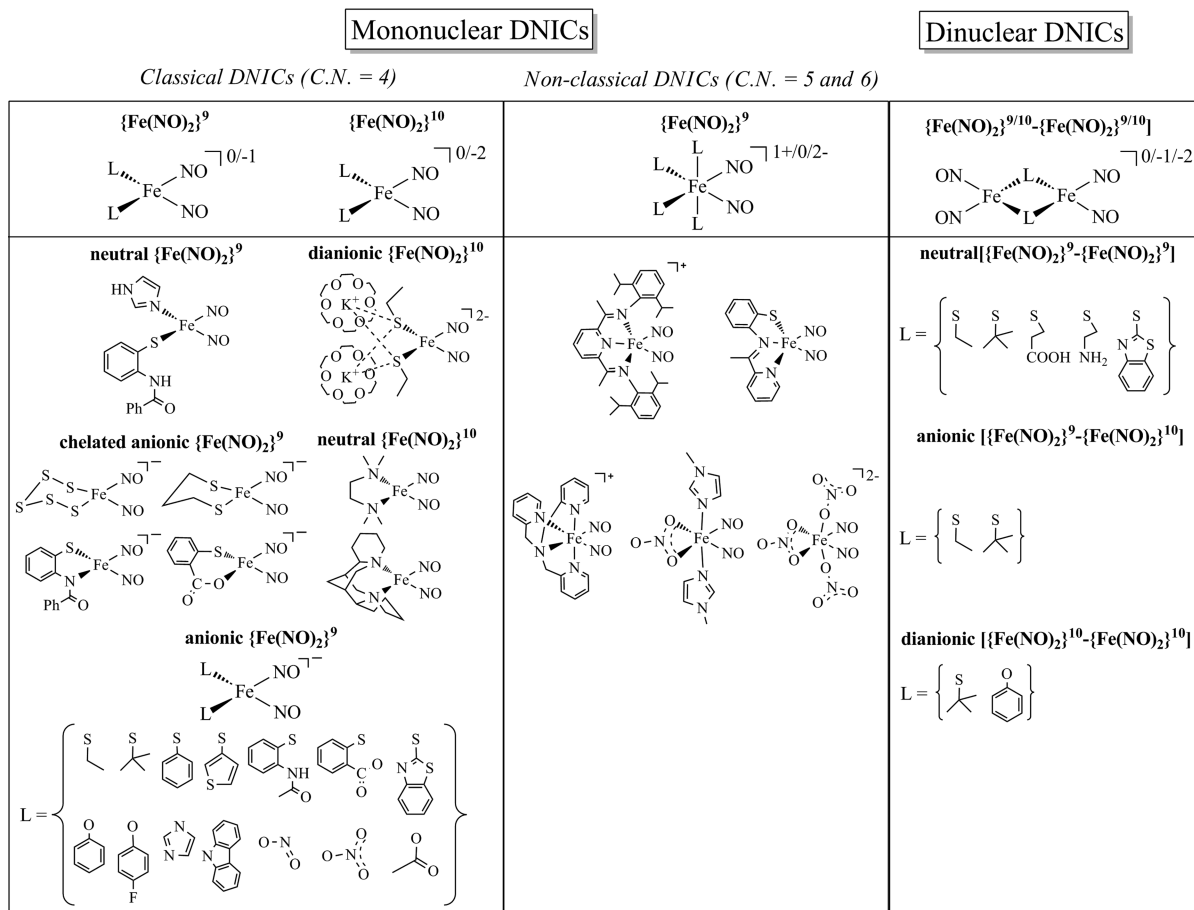
Scheme 1^{11,12,21}



pathways of dinuclear DNICs modulated by the bridging ligands and the nature of nucleophiles have been demonstrated: (1) bridged-thiolate cleavage to generate neutral S_{Nim} - and anionic S_{S} -bound mononuclear DNICs from the reaction of imidazole (σ -donor)/thiolate (π -donor) and dinuclear DNICs, respectively;^{10,11} (2) deprotonation of amide and carboxylic acid groups by phenolate (weak base) to yield the anionic S_{Namide} - and $\text{S}_{\text{O}_{\text{COO}}}$ -chelated mononuclear DNICs, respectively;¹¹ (3) electron reduction to produce the one- or two-electron reduced $[\{\text{Fe}(\text{NO})_2\}^{9/10}-\{\text{Fe}(\text{NO})_2\}^{9/10}]$ dinuclear DNICs.^{12,21} By adopting the developed synthetic methodologies, the mononuclear $\{\text{Fe}(\text{NO})_2\}^{9/10}$ DNICs and dinuclear $[\{\text{Fe}(\text{NO})_2\}^{9/10}-\{\text{Fe}(\text{NO})_2\}^{9/10}]$ DNICs with biologically relevant S/O/N ligation modes were successfully synthesized and characterized by single-crystal X-ray crystallography (Scheme 2).^{10–24} The biomimetic studies on interconversion of the structurally well-defined DNICs allow us to determine the binding affinity of biologically relevant ligands toward the $\{\text{Fe}(\text{NO})_2\}^9$ motif to be thiolate (SR^-) > imidazolate (Im^-) > phenolate (OPh^-) > carboxylate (COO^-) > nitrite (NO_2^-) > nitrate (NO_3^-). The order of binding affinity of these ligands toward the $\{\text{Fe}(\text{NO})_2\}^9$ core may provide a general guideline for the possible ligation modes of DNICs under the presence of multiple coordinating amino acid residues in biological environments.¹⁵ In addition to the classical four-coordinate DNICs, the nonclassical DNICs with either five- or six-coordinate ligands were found to be stabilized by multidentate ligands including bidentate (the κ^2 -ONO binding mode from nitrite; the κ^2 - O_2NO binding mode from nitrate),^{14,17,20,25} tridentate (N_3 donor ligation from iPrPDI where $\text{iPrPDI} = 2,6\text{-}[\text{2,6-}^{\text{iPr}}\text{Pr}_2\text{-C}_6\text{H}_3\text{N}=\text{CMe}]_2\text{C}_3\text{H}_3\text{N}$); N_2S donor ligation from PyImiS where $\text{PyImiS} = 2\text{-}[2\text{-}(\text{C}_5\text{H}_4\text{N})\text{CMe}=\text{N}]\text{C}_6\text{H}_4\text{S}$), and tetradentate (N_4 donor ligation from TPA where $\text{TPA} = 2\text{-}[\text{CH}_2\text{-C}_5\text{H}_4\text{N}]_3\text{N}$) ligands, which extend the molecular geometries of DNICs from conventional tetrahedral ($\text{CN} = 4$) to square pyramidal and trigonal bipyramidal ($\text{CN} = 5$) and octahedral ($\text{CN} = 6$).¹⁹ Interestingly, the homoleptic nitrosyl $\{\text{Fe}(\text{NO})_2\}^9$ DNIC, $[\text{Fe}(\text{NO})_4]^-$ with two nitroxyls attached to a delocalized $\{\text{Fe}(\text{NO})_2\}^9$ motif, was also synthesized.²⁶ The comprehensive biomimetic DNIC models with biologically relevant ligation modes and molecular geometries provide the foundation to establish the spectroscopic references (^{15}N NMR,

Scheme 2

Dinitrosyl Iron Complexes (DNICs)



EPR, IR, nuclear resonance vibrational spectroscopy (NRVS), and X-ray absorption (XAS) and X-ray emission spectroscopy (XES)) that are accessible in biological environments to signify the existence and monitor the transformation of the various DNICs in biological systems. Furthermore, the roles of coordinated ligands and molecular geometry of DNICs in modulating their electronic structures and chemical reactivity could also be investigated.

SPECTROSCOPIC REFERENCES AND ELECTRONIC STRUCTURES OF DNICs

The spectroscopic methods covering the energies from radio frequency to X-ray provide comprehensive descriptions of electronic structure associated with the local environment of nuclear spin, the distribution of unpaired electrons, the vibrational motion of molecules, and the oxidation states of atoms. Specifically, the local environment of atoms possessing nuclear spin $\geq 1/2$ is characterized by chemical shift (δ) in NMR. The distribution of unpaired electrons under the magnetic field is parametrized by g -value and hyperfine splitting in EPR. The types of molecular movements and the strengths of chemical bonds are related to vibrational frequencies in IR spectroscopy. The oxidation state of atoms can be probed by the energies of core-level electronic transitions obtained from K-edge X-ray absorption (XAS) and X-ray emission spectroscopy (XES). Beyond the static portrait derived from single-

crystal X-ray crystallography, the characteristic features of complementary spectroscopic methods provide credible guidance to uncover molecular geometries as well as coordination environments in a dynamic regime and to provide insights to electronic structures dictating chemical reactivity and biological functions.

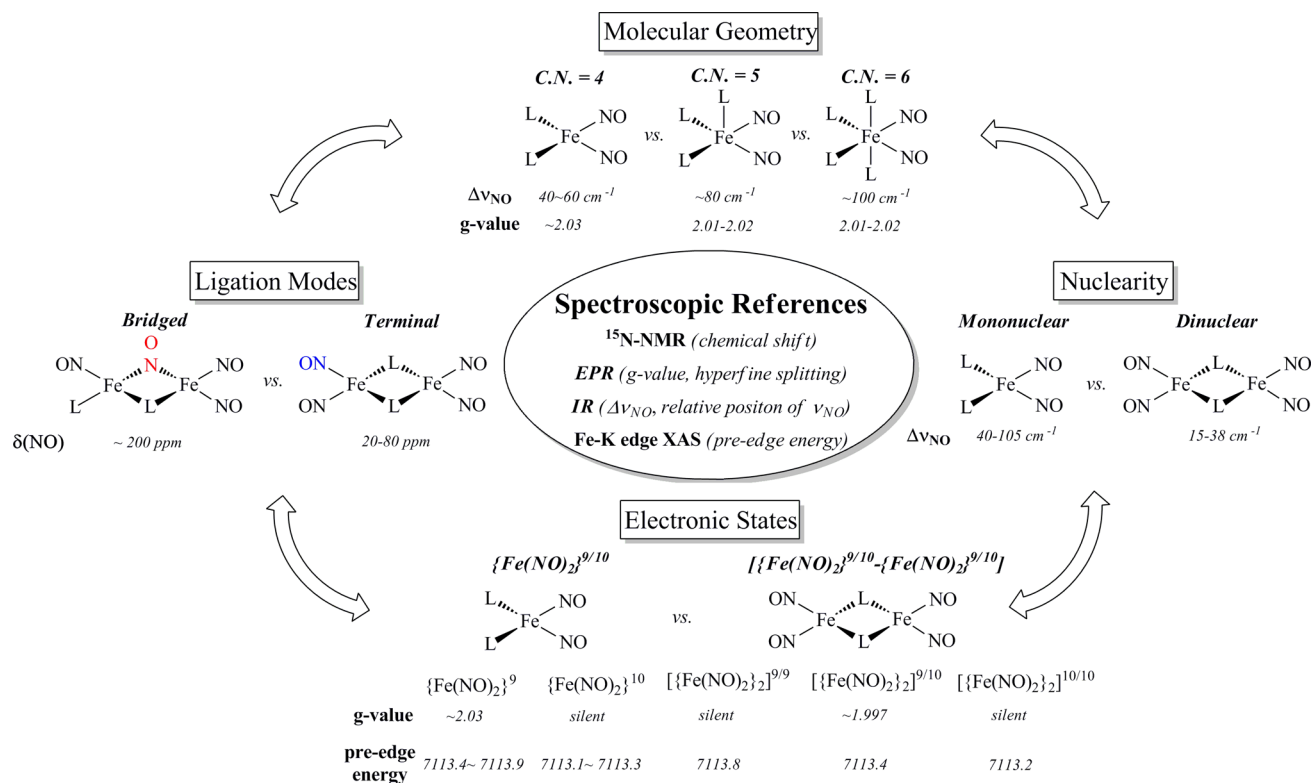
SPECTROSCOPIC REFERENCES TO DISCRIMINATE DNICs

Combinations of different spectroscopic features unique to the geometric and electronic structures offer a superior level of uncovering the molecular identity in complex environments. The spectroscopic measurements of structurally well-defined biomimetic DNIC models indicate that the chemical shift of ^{15}N NMR,^{23,27} g -value and hyperfine splitting patterns in EPR,^{17,19} separation of ν_{NO} in IR,^{17,19-21,28,29} and pre-edge energy in Fe/S K-edge XAS^{15,21,28,30} could be utilized to establish the spectroscopic references for discriminating molecular geometries (tetrahedral vs square pyramidal vs octahedral), ligation modes (terminal vs bridging), nuclearity (mononuclear vs dinuclear), and electronic states ($\{\text{Fe}(\text{NO})_2\}^{9/10}$ vs $[\{\text{Fe}(\text{NO})_2\}^{9/10}-\{\text{Fe}(\text{NO})_2\}^{9/10}]$) of DNICs (Scheme 3).

Molecular Geometry

Four-coordinate and five- or six-coordinate DNICs exhibit characteristic g -values of ~ 2.03 and $\sim 2.012-2.018$ with

Scheme 3



$A(^{14}\text{NO})/A(^{15}\text{NO}) \approx 0.7$, respectively.¹⁹ Furthermore, $\Delta\nu_{\text{NO}}$ values ($\Delta\nu_{\text{NO}}$ = the separation of NO stretching frequencies) of four-coordinate DNICs fall into the range around 40–60 cm^{-1} . The $\Delta\nu_{\text{NO}}$ values of five-coordinate and six-coordinate mononuclear DNICs have been determined to be ~80 and ~100 cm^{-1} , respectively. Therefore, a combination of g-value and $\Delta\nu_{\text{NO}}$ allow us to differentiate molecular geometries among four-, five-, and six-coordinate DNICs.

Ligation Modes

The terminal and bridging binding modes of nitric oxide toward $[\text{Fe}(\text{NO})_2]$ core exhibit distinct ^{15}N chemical shift (δ). That is, terminal NO and bridging NO of dinuclear DNICs show diagnostic chemical shift around 20–80 ppm and ~200 ppm in ^{15}N NMR,^{23,27} respectively.

Nuclearity

On the basis of IR ν_{NO} spectra of the biomimetic DNICs, the mononuclear and dinuclear DNICs display characteristic $\Delta\nu_{\text{NO}}$ around 40–105 cm^{-1} and 15–38 cm^{-1} , respectively. These features provide definitive spectroscopic evidence to distinguish the nuclearity of DNICs.^{11,17,19,21}

Electronic States

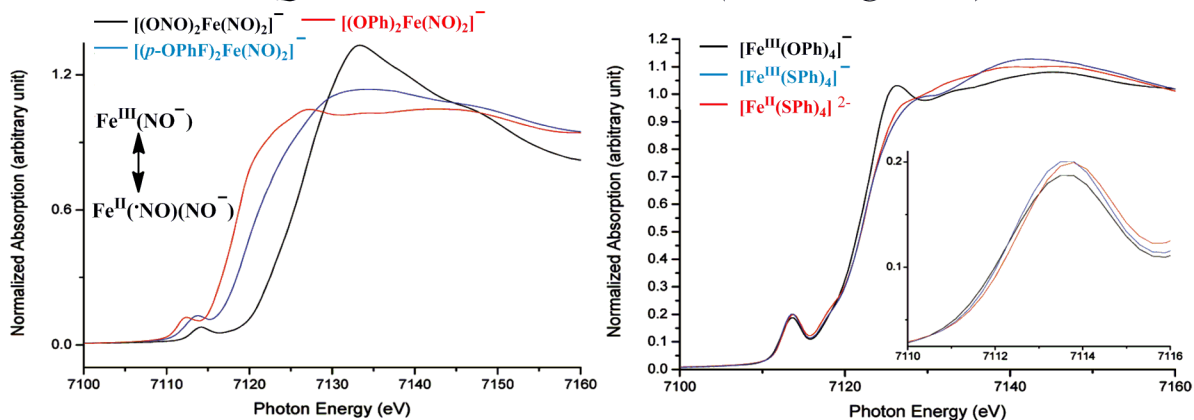
The mononuclear DNICs, in general, show reversible one-electron redox couple shuttling between $\{\text{Fe}(\text{NO})_2\}^9$ and $\{\text{Fe}(\text{NO})_2\}^{10}$ electronic states, and the dinuclear DNICs consisting of two $[\text{Fe}(\text{NO})_2]$ motifs display three distinct $\{[\text{Fe}(\text{NO})_2]_2\}^{9/10}-\{[\text{Fe}(\text{NO})_2]_2\}^{9/10}$ electronic states.^{12,21} In contrast to the EPR-silent dinuclear $[\{[\text{Fe}(\text{NO})_2]_2\}^9-\{[\text{Fe}(\text{NO})_2]_2\}^9]$ DNICs, the reduced-form dinuclear $[\{[\text{Fe}(\text{NO})_2]_2\}^9-\{[\text{Fe}(\text{NO})_2]_2\}^{10}]$ DNICs display the diagnostic axial EPR signal of $g_{\perp} \approx 2.009$, $g_{\parallel} \approx 1.965$ at 77 K. Monitoring the changes of EPR signal and the shift of ν_{NO} (decrease by ~100 cm^{-1} for one-electron reduction of mononuclear and dinuclear DNICs), the

EPR-silent mononuclear $\{\text{Fe}(\text{NO})_2\}^{10}$ and double-reduced $[\{[\text{Fe}(\text{NO})_2]_2\}^{10}-\{[\text{Fe}(\text{NO})_2]_2\}^{10}]$ DNICs could be identified. In addition, the combination of aqueous IR ν_{NO} and EPR spectra can serve as an efficient tool to characterize and distinguish chelate- or monodentate-cysteine-containing peptide-bound DNICs/RREs.^{28,29} Additional evidence is provided by the pre-edge energy of Fe K-edge XAS showing the characteristic electronic transitions around 7113.4–7113.9 eV and 7113.1–7113.3 eV for $\{\text{Fe}(\text{NO})_2\}^9$ and $\{\text{Fe}(\text{NO})_2\}^{10}$ DNICs, respectively.^{15,21} Also, S K-edge pre-edge absorption energy and pattern are useful as criteria to discriminate and characterize mononuclear and dinuclear DNICs containing bridged thiolate or sulfide.³⁰

■ DETERMINATION OF THE Fe AND NO OXIDATION STATES IN DNICs AND MONONITROSYL IRON COMPLEXES (MNICs)

The assignment of Fe and NO oxidation states in Fe–nitrosyl complexes has been complicated by the noninnocent nature resulting from similar energy levels between the Fe 3d manifold and low-lying NO π^* orbitals.³¹ Although Enemark–Feltham notation ($[\text{Fe}(\text{NO})_x]^n$) provides a general way to describe the electronic structure of Fe–nitrosyl complexes,⁹ the unambiguous determination of Fe and NO oxidation states is essential for elucidating physical properties and chemical reactivity. The core-level spectroscopic methods including Fe/S K-edge XAS^{15,21,30} and valence to core (V2C) Fe $K\beta$ XES³² coupled with *ab initio* DFT calculations provide direct probes for qualitative and quantitative assignments of Fe and NO oxidation states in Fe–nitrosyl complexes.³³ Complementarily, the detailed vibrational spectroscopic studies (IR, rR, NRVS) coupled with DFT calculations have been demonstrated to directly probe the strengths of Fe–NO and N–O bonds in

Qualitative Oxidation States (Fe K-edge XAS)



Quantitative Oxidation States (V2C Fe Kβ XES)

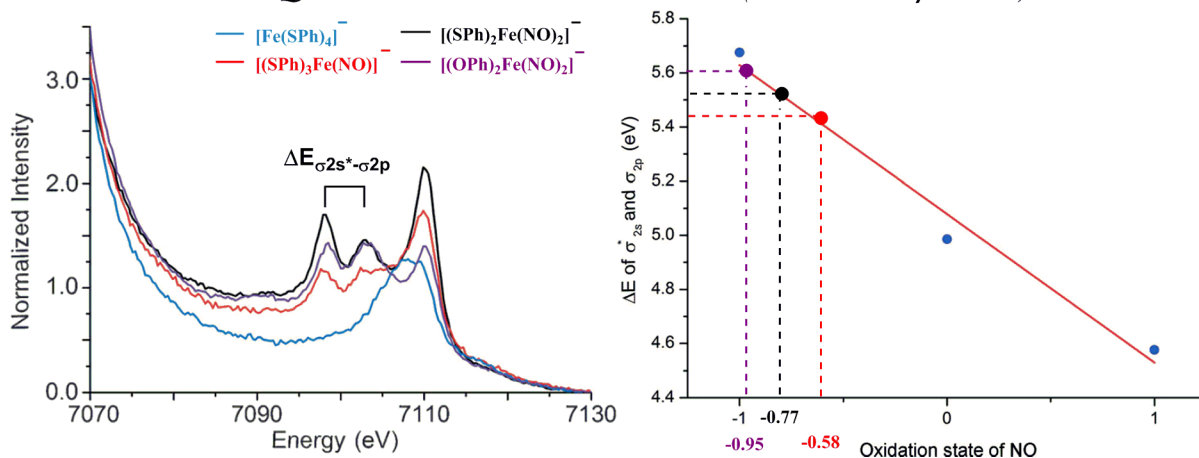


Figure 1. Fe K-edge XAS of $[(\text{ONO})_2\text{Fe}(\text{NO})_2]^-$, $[(\text{PhO})_2\text{Fe}(\text{NO})_2]^-$, and $[(p\text{-FPhO})_2\text{Fe}(\text{NO})_2]^-$; V2C Fe K β XES spectra of $[(\text{PhS})_3\text{Fe}(\text{NO})]^-$, $[(\text{PhO})_2\text{Fe}(\text{NO})_2]^-$, and $[(\text{PhS})_2\text{Fe}(\text{NO})_2]^-$ (note that $[\text{Fe}^{\text{III}}(\text{OPh})_4]^-$ / $[\text{Fe}^{\text{III}}(\text{SPh})_4]^-$ and $[\text{Fe}^{\text{II}}(\text{SPh})_4]^{2-}$ were used as Fe^{II} and Fe^{III} standard in Fe K-edge XAS, respectively).^{15,26}

Fe–NO complexes providing the insights of Fe–NO bonding interactions upon the changes of redox states, molecular geometry, and coordination environments.^{34,35}

The qualitative determination of the electronic structure of mononuclear $\{\text{Fe}(\text{NO})_2\}^9$ DNICs was derived from the pre-edge energy of Fe K-edge XAS. The pre-edge energies of tetrahedral $\{\text{Fe}(\text{NO})_2\}^9$ DNICs with various ligation modes were determined to be $\sim 7113.4\text{--}7113.9$ eV which fall into the pre-edge energy between Fe^{II} (7112.5 eV for $[\text{Fe}^{\text{II}}(\text{SPh})_4]^{2-}$) and Fe^{III} standards (7113.8 eV for $[\text{Fe}^{\text{III}}(\text{SPh})_4]^-$ and 7114.2 eV for $[\text{Fe}^{\text{III}}(\text{OPh})_4]^-$) (Figure 1).¹⁴ Therefore, the electronic structure of $\{\text{Fe}(\text{NO})_2\}^9$ DNICs was qualitatively described as a resonance hybrid of $\{\text{Fe}^{\text{II}}(\text{NO})(\text{NO}^-)\}^9$ and $\{\text{Fe}^{\text{III}}(\text{NO}^-)_2\}^9$ electronic states. On the basis of DFT calculations, the contributions from two resonance forms are further modulated by the nature of coordinated ligands. Specifically, the coordination of “hard” O-containing ligands tends to polarize the $\{\text{Fe}(\text{NO})_2\}^9$ core to possess more $\{\text{Fe}^{\text{III}}(\text{NO}^-)_2\}^9$ character than the corresponding DNICs with “soft” S,S-ligation modes. In addition, combination of S K-edge pre-edge and thiolate peak energies establishing the relative energy of the Fe_{3d} manifold orbitals also supported the $\{\text{Fe}^{\text{III}}(\text{NO}^-)_2\}^9$ electronic structure for $[(\text{EtS})_2\text{Fe}(\text{NO})_2]^-$ and the $[\{\text{Fe}^{\text{III}}(\text{NO}^-)_2\}^9 - \{\text{Fe}^{\text{III}}(\text{NO}^-)_2\}^9]$ core for $[(\mu\text{-EtS})\text{Fe}(\text{NO})_2]_2$.³⁰ The extensive DFT calculations on $\{\text{Fe}(\text{NO})_2\}^9$ and $\{\text{Fe}(\text{NO})_2\}^{10}$ DNICs

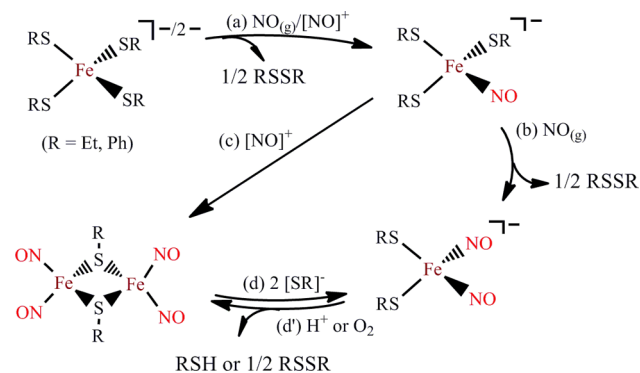
calibrated by their experimental isomer shifts (δ) and quadrupole splittings (ΔE_Q) of ^{57}Fe Mössbauer spectroscopy as well as NO stretching frequencies are also consistent with the resonance hybrid of $\{\text{Fe}^{\text{III}}(\text{NO}^-)_2\}^9$ and $\{\text{Fe}^{\text{II}}(\text{NO})(\text{NO}^-)\}^9$ description in $\{\text{Fe}(\text{NO})_2\}^9$ DNICs derived from Fe/S K-edge XAS. In addition, the electronic structure of $\{\text{Fe}(\text{NO})_2\}^{10}$ DNICs is further suggested as $\{\text{Fe}^{\text{II}}(\text{NO}^-)_2\}^{10}$ resulting from high spin Fe^{II} ($S = 2$) antiferromagnetically coupled with two triplet NO^- ligands.^{31,36}

Recently, the NO redox level in Fe–nitrosyl complexes has been quantitatively determined by the newly developed V2C Fe K β XES (Figure 1).³³ Unprecedentedly, the oxidation states of the coordinated NO of $[(\text{PhS})_3\text{Fe}(\text{NO})]^-$, $[(\text{PhS})_2\text{Fe}(\text{NO})_2]^-$, and $[(\text{PhO})_2\text{Fe}(\text{NO})_2]^-$ were quantitatively determined to be -0.58 ± 0.18 , -0.77 ± 0.18 , and -0.95 ± 0.18 , respectively, derived from the equation $\Delta E_{\sigma_{2s^*} - \sigma_{2p}} = -0.550 \times (\text{redox level of NO}) + 5.079$ where $\Delta E_{\sigma_{2s^*} - \sigma_{2p}}$ represents the energy separation between σ_{2s^*} and σ_{2p} orbitals of Fe-bound nitric oxide. The consistency of qualitative Fe K-edge XAS and quantitative V2C Fe K β XES measurements unequivocally settle the assignment of Fe^{III} and NO^- redox level and solidify the critical role of coordinated ligands in modulating the electronic structure of $\text{Fe}(\text{NO})_2$ core in DNICs.

DEGRADATION OF [Fe–S] CLUSTERS IN THE PRESENCE OF NO AND REPAIR PROCESSES

The most abundant nitric oxide-derived cellular adducts, protein-bound DNICs and RREs (Roussin's red esters), are demonstrated to be mainly derived from nitrosylation of the cellular and chelatable iron pool and [Fe–S] proteins.^{37–40} In the repair of NO-modified [2Fe–2S] and [4Fe–4S] clusters, protein-bound DNICs and RREs can be directly transformed back to the [2Fe–2S] of SoxR by cysteine desulfurase (IscS, S-donor protein) and L-cysteine *in vitro* with no need for the addition of iron and back to the [4Fe–4S] of endonuclease III or DNA-damage-inducible protein (DinG) under the presence of external ferrous ion, respectively.^{39,41} The ubiquity of DNICs and RREs in biology provides a compelling reason to search for mechanistic understanding of degradation and repair of [Fe–S] clusters by models that inform the contributions of the {Fe(NO)₂} motif to the overall interconvertible processes.

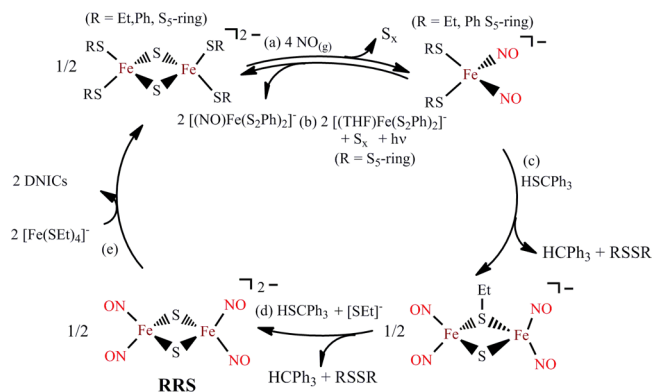
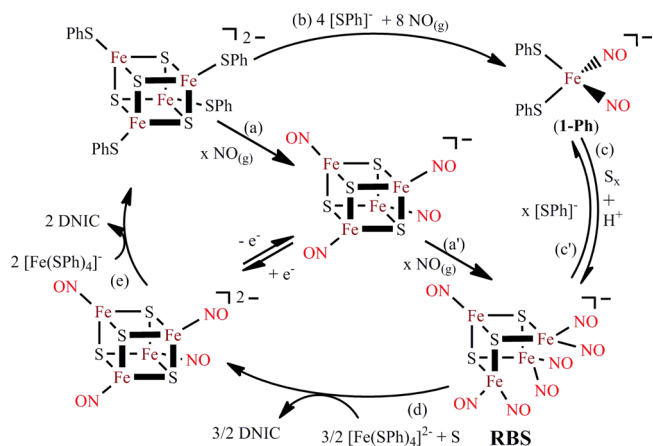
As shown in Scheme 4, upon nitrosylating the biomimetic oxidized and reduced form rubredoxin [Fe(SR)₄]^{–2–} (R = Et,

Scheme 4⁴²

Ph), {Fe(NO)₂}⁹, [(RS)₂Fe(NO)₂][–], is generated via {Fe(NO)}⁷ mononitrosyl iron complexes (MNICs), [(RS)₃Fe(NO)][–]. Intriguingly, DNICs, [(RS)₂Fe(NO)₂][–], and RREs, [(RS)₂Fe(NO)]₂, are chemically interconvertible by protonation of {Fe(NO)₂}⁹ DNICs and thiolate-nucleophilic cleavage of RREs, respectively.⁴²

The [Fe₂S₂(SR)₄]^{2–}-to-DNIC-to-[(NO)₄Fe₂(μ-SR)(μ-S)][–]-to-[(NO)₂Fe(μ-S)]₂^{2–} conversion provides a facile pathway for repair of the NO-modified [Fe–S] clusters back to the original biomimetic [Fe–S] clusters via reductive sulfide transfer of HSCPh₃ followed by NO radical–thiyl radical exchange (or nitroxyl–thiolate exchange) reaction (Scheme 5).^{43,44}

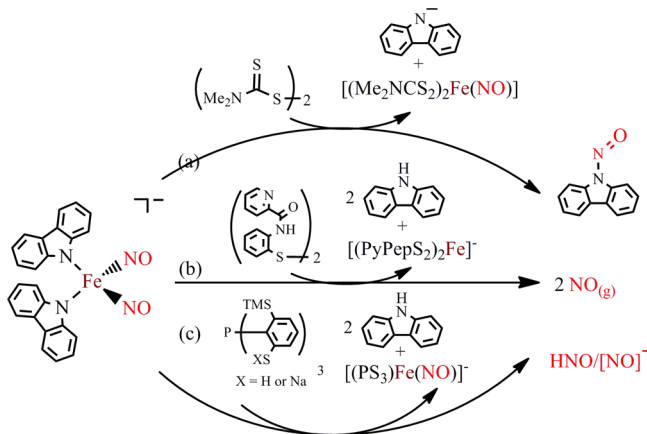
Repair of DNICs derived from nitrosylation of a biomimetic [4Fe–4S]-cluster, [Fe₄S₄(SPh)₄]^{2–}, back to the original [4Fe–4S] cluster can be achieved via preassembled cluster [Fe₄S₄(NO)₄]^{2–} generated in the course of intermolecular NO radical–thiyl radical exchange (or nitroxyl–thiolate exchange) between [Fe₄S₃(NO)₇]^{2–} (reduced-form Roussin's black salt (RBS)) and [Fe(SPh)₄]^{2–} accompanied by oxidative addition of sulfur. The sequential capture of [Fe(SPh)₄]^{2–} by [Fe₄S₄(NO)₄]^{2–} yields [Fe₄S₄(SPh)₄]^{2–} and DNIC (Scheme 6).⁴⁵

Scheme 5^{43,44}Scheme 6⁴⁵

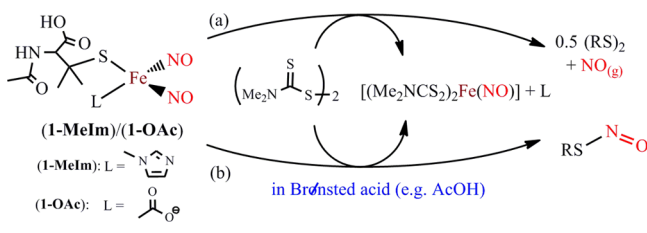
TRANSFORMATION OF DNICs INTO S-NITROSOTHIOL (RSNO)/N-NITROSAMINE (R₂NNO) AND NO⁺/NO[•]/NO[–]

The redox-interrelated forms of nitric oxide (NO⁺/NO[•]/NO[–]) have been demonstrated to play vital roles in a variety of physiological and pharmacological functions, such as vasodilation, apoptosis, and antitumor activity.^{46,47} In particular, a dinuclear DNIC containing glutathione has been developed as a commercial hypotensive drug (pharmacological name: Oxacom).⁴⁶ DNICs not only donate NO(g) or nitroxyl (NO[–]) to metal active sites, but also behave as [NO]⁺-donor for S-nitrosation or N-nitrosation.^{48,49} In addition to the redox levels of the intrinsic NO ligands of DNICs regulated by the coordinated ligands, as shown in Scheme 7, release of the distinct NO redox-interrelated forms (NO⁺/NO[•]/NO[–]), derived from the unique {Fe(NO)₂}⁹ DNIC [(NO)₂Fe(C₁₂H₈N)₂][–] (C₁₂H₈N = carbozolate), are modulated by the distinct incoming substitution ligands with oxidizing capability and mediated or driven by the formation of {Fe(NO)}⁷ MNIC.¹⁶

Recently, several reports have suggested that the protein-bound DNIC is a dominant species for producing cellular protein-bound S-nitrosothiols (RSNOs) via an O₂-independent pathway.⁴⁸ In biomimetic study, in contrast to the transformation of one-thiolate-containing {Fe(NO)₂}⁹ DNIC [(NO)₂Fe(1-MeIm)(SR)][–] (R = alkyl) into {Fe(NO)}⁷ MNIC [(NO)Fe(S₂CNMe₂)₂][–] along with the release of NO triggered by bis(dimethylthiocarbamoyl) disulfide ([DTC]₂), the transformation of the Brønsted acid-stable one-thiolate-

Scheme 7¹⁶

containing $\{\text{Fe}(\text{NO})_2\}^9$ DNIC $[(\text{NO})_2\text{Fe}(\text{1-MeIm})(\text{SR})]^-$ into RSNO promoted by the incoming ligand $[\text{DTC}]_2$ demonstrates that Brønsted acid is a prerequisite to trigger DNIC-to-RSNO conversion accompanied by the transformation of $\{\text{Fe}(\text{NO})_2\}^9$ $[(\text{NO})_2\text{Fe}(\text{1-MeIm})(\text{SR})]^-$ into $\{\text{Fe}(\text{NO})\}^7$ $[(\text{NO})\text{Fe}(\text{S}_2\text{CNMe}_2)_2]^-$ (Scheme 8).¹⁸ The results of this model study

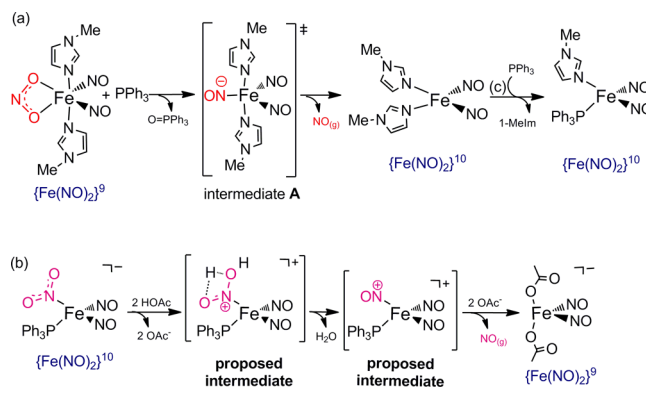
Scheme 8¹⁸

may rationalize that the known Cys–SNO sites of protein derived from DNICs are characterized to locate near acidic and basic motifs (i.e., Glu/Asp/His/Lys/Arg at a distance of 3–9 Å).¹⁸

NITRITE/NITRATE ACTIVATION PRODUCING NO REGULATED BY $\{\text{Fe}(\text{NO})_2\}^{9/10}$ DNICs AND $\{\text{Fe}(\text{NO})\}^{6/7}$ MNICs

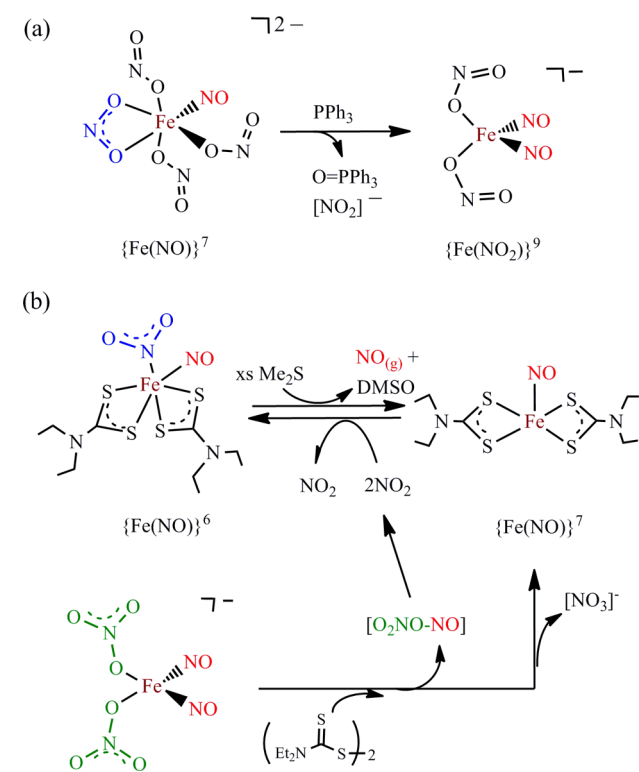
Nitrite ($[\text{NO}_2]^-$) and nitrate ($[\text{NO}_3]^-$), ubiquitous molecules *in vivo*, are known to serve as intravascular NO storage and transport species to transduce NO bioactivity in blood circulation. The nitrate \rightarrow nitrite \rightarrow NO pathway is emerging as an important mediator of cell signaling, blood flow regulation, and tissue responses during physiological and pathological hypoxia.⁵⁰ Although heme iron and copper have been identified as active sites of nitrite reductases (NiRs),⁵¹ non-heme $[\text{4Fe-4S}]$ clusters and deoxyhemerythrin under the treatment of nitrite also trigger nitrite reduction to generate DNIC and deoxyhemerythrin-MNIC, individually.^{52,53}

As shown in Scheme 9, a model study demonstrates that the distinct electronic structures of $\{\text{Fe}(\text{NO})_2\}^{9/10}$ DNICs ($\{\text{Fe}(\text{NO})_2\}^9$ vs $\{\text{Fe}(\text{NO})_2\}^{10}$ motifs) play key roles in modulating nitrite binding modes to trigger nitrite-to-nitroxyl-to-nitric oxide conversion and nitrite-to-nitrosonium-to-nitric oxide conversion, respectively. Specifically, the nonbiological PPh_3 triggers O atom abstraction of the O-bound chelating nitrito of $\{\text{Fe}(\text{NO})_2\}^9$ $[(\text{1-MeIm})_2(\kappa^2\text{-NO}_2)\text{Fe}(\text{NO})_2]$ to produce $\text{NO}(\text{g})$ along with the formation of $\{\text{Fe}(\text{NO})_2\}^{10}$ $[(\text{1-MeIm})(\text{PPh}_3)]^-$

Scheme 9^{14,17}

$\{\text{Fe}(\text{NO})_2\}^9$ (Scheme 9a).^{14,17,54,55} In comparison, protonation of N-bound nitro of $\{\text{Fe}(\text{NO})_2\}^{10}$ $[(\text{PPh}_3)(\eta^1\text{-NO}_2)\text{Fe}(\text{NO})_2]$ by HOAc leads to the generation of $\text{NO}(\text{g})$ and $\{\text{Fe}(\text{NO})_2\}^9$ $[(\text{AcO})_2\text{Fe}(\text{NO})_2]^-$ (Scheme 9b).¹⁷

Mononitrosyl iron complexes (MNICs) also display nitrite-reductase activity. MNICs $[(\kappa^1\text{-ONO})_3(\kappa^2\text{-O}_2\text{N})\text{Fe}(\text{NO})]^{2-}$ and $[(\text{Et}_2\text{NCS})_2(\eta^1\text{-NO}_2)\text{Fe}(\text{NO})]$ are considered as reduced and oxidized forms of MNICs ($\{\text{Fe}(\text{NO})\}^7$ vs $\{\text{Fe}(\text{NO})\}^6$); the binding modes of nitrite exhibit O-bound nitrito for $\{\text{Fe}(\text{NO})\}^7$ MNIC $[(\kappa^1\text{-ONO})_3(\kappa^2\text{-O}_2\text{N})\text{Fe}(\text{NO})]^{2-}$ and N-bound nitro for $\{\text{Fe}(\text{NO})\}^6$ MNIC $[(\text{Et}_2\text{NCS})_2(\eta^1\text{-NO}_2)\text{Fe}(\text{NO})]$ (Scheme 10). The nitrite reduction of MNICs $[(\kappa^1\text{-ONO})_3(\kappa^2\text{-O}_2\text{N})\text{Fe}(\text{NO})]^{2-}$ and $[(\text{Et}_2\text{NCS})_2(\eta^1\text{-NO}_2)\text{Fe}(\text{NO})]$ is achieved by means of O atom abstraction to yield $\{\text{Fe}(\text{NO})_2\}^9$ $[(\kappa^1\text{-ONO})_2\text{Fe}(\text{NO})_2]^-$ and $\{\text{Fe}(\text{NO})\}^7$ $[(\text{Et}_2\text{NCS})_2\text{Fe}(\text{NO})]$ along with NO via the proposed intermediates containing nitroxyl-coordinate ligands, respectively.^{17,20}

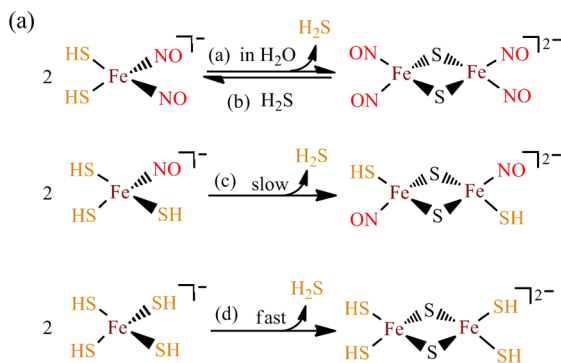
Scheme 10²⁰

Compared with the N- and S-nitrosation of the coordinate N- and S-ligand of DNIC triggered by $(\text{Me}_2\text{NCS}_2)_2$ (Schemes 7a and 8b), disulfide $((\text{S}_2\text{CNEt}_2)_2)$ triggering “NO₃-nitrosation” of $[(\kappa^1\text{-ONO}_2)_2\text{Fe}(\text{NO})_2]^-$ and subsequent NO₂ addition to $[(\text{Et}_2\text{NCS}_2)_2\text{Fe}(\text{NO})]$ followed by Me₂S-promoted oxygen-atom transfer of $\{\text{Fe}(\text{NO})\}^6$ $[(\text{Et}_2\text{NCS}_2)_2(\eta^1\text{-NO}_2)\text{Fe}(\text{NO})]$ lead to the formation of complex $[(\text{Et}_2\text{NCS}_2)_2\text{Fe}(\text{NO})]$ along with release of NO (Scheme 10b).²⁰ This model study shows that $\{\text{Fe}(\text{NO})_2\}^9$ DNIC $[(\kappa^1\text{-ONO}_2)_2\text{Fe}(\text{NO})_2]^-$ acts as an active center to modulate nitrate-to-nitrite-to-NO conversion promoted by disulfides.

■ DNICs FOR H₂S STORAGE

In addition to the diatomic NO, it has been recently proposed that hydrogen sulfide (H₂S) also functions as an endogenously produced biological signaling molecule in the cardiovascular and nervous systems. The heme iron-mediated cross-talk between NO and H₂S was suggested as a potential pathway for the generation of HSNO.⁵⁶ Efforts to understand the cooperative interaction of H₂S and NO in biological environments continues to be a challenge, highlighting the importance of the interplay between DNICs and H₂S. As shown in Scheme 11, $[(\text{HS})_2\text{Fe}(\text{NO})_2]^-$, $[(\text{HS})_3\text{Fe}(\text{NO})]^-$, and $[\text{Fe}(\text{SH})_4]^-$,

Scheme 11²²



obtained from reactions of H₂S and $[(\text{EtS})_2\text{Fe}(\text{NO})_2]^-$ / $[(\text{EtS})_3\text{Fe}(\text{NO})]^-$ / $[\text{Fe}(\text{SEt})_4]^-$, respectively, spontaneously dimerized into the structurally characterized $[(\text{NO})_2\text{Fe}(\mu\text{-S})]_2^{2-}$, $[(\text{NO})(\text{HS})\text{Fe}(\mu\text{-S})]_2^{2-}$, and $[\text{Fe}_2(\mu\text{-S})_2(\text{SH})_4]^{2-}$ along with release of H₂S probed by NBD-SCN (NBD = nitrobenzofurazan) in protic solvent (H₂O, MeOH) at room temperature.²² DFT computation and the experimental reduction potentials ($E_{1/2}$) of complexes $[(\text{HS})_n\text{Fe}(\text{NO})_m]^-$ ($n = 4, 3, 2; m = 0, 1, 2$) and $[(\text{HS})_n(\text{NO})_m\text{Fe}(\mu\text{-S})]_2^{2-}$ ($n = 0, 1, 2; m = 2, 1, 0$) suggest that triplet NO⁻ bound to the $[(\text{HS})\text{Fe}]$ motif acts as an effective regulator to reduce the Z_{eff} of iron to prevent the reductive elimination of the coordinated hydrosulfide ligands. In contrast to $[(\text{HS})_2\text{Fe}(\mu\text{-S})]_2^{2-}$ slowly converting into $[\text{Fe}_4\text{S}_4(\text{SH})_4]^{2-}$, the stabilization of $[(\text{HS})(\text{NO})\text{Fe}(\mu\text{-S})]_2^{2-}$ and $[(\text{NO})_2\text{Fe}(\mu\text{-S})]_2^{2-}$ suggest that $[(\text{HS})(\text{NO})\text{Fe}(\mu\text{-S})]_2^{2-}$ and $[(\text{NO})_2\text{Fe}(\mu\text{-S})]_2^{2-}$ are tailored to preserve the $[\text{Fe}^{\text{III}}(\mu\text{-S})_2\text{Fe}^{\text{III}}]$ oxidation state, modulated by the NO-coordinate ligands. These results signify that the hydrosulfide-coordinated DNICs and MNICs may serve not only for H₂S storage and transport but also as an alternative sulfur source for the synthesis of $[\text{Fe}-\text{S}]$ clusters.^{22,57}

■ CELLULAR PERMEATION PATHWAYS OF DNICs/RREs FOR SUBSEQUENT PROTEIN S-NITROSYLATION

The development of a NO-releasing agent for physiological use is a significant goal. It is known that the physiologically beneficial concentration of nitric oxide is in the picomolar to nanomolar range. Much current research is directed toward the development of DNICs/RREs capable of controlled delivery and release of NO for specific pharmacological applications. EPR spectroscopic analysis demonstrated that the structurally characterized, water-soluble RRE $[(\text{NO})_2\text{Fe}(\text{SC}_2\text{H}_4\text{COOH})]_2$ may permeate cell membranes and then convert into protein- and cysteine-bound DNICs to induce NO-dependent upregulation of cellular heat shock protein 70 (HSP70), and *in vivo* protein S-nitrosylation. The detection of intracellular $\{\text{Fe}(\text{NO})_2\}^9$ DNICs in the absence of serum and L-cysteine also supports the direct transport of $[(\text{HOOCH}_2\text{C}_2\text{S})\text{Fe}(\text{NO})_2]_2$ RRE into cells accompanied by its transformation into $\{\text{Fe}(\text{NO})_2\}^9$ protein- and cysteine-bound DNICs. The capability of the long half-life NO-donor $[(\text{HOOCH}_2\text{C}_2\text{S})\text{Fe}(\text{NO})_2]_2$ to induce HSP70 overexpression may signify its potential to exert a cardioprotective effect in vascular endothelial cells.¹³

■ CONCLUSION AND PERSPECTIVES

The research on DNICs, reflecting the merit of bioinorganic chemistry, integrates interdisciplinary efforts consisting of biomimetic synthesis, inorganic spectroscopy, molecular catalysis, and biological applications to investigate their versatile molecular geometries and electronic structures as well as the development of spectroscopic references for tracking the existence and transformation of DNICs. The fundamental knowledge was progressively conveyed to provide insights on nitrite/nitrate activation generating nitric oxide and selective nitrosylation (NO⁺, NO[•], or NO⁻) of biologically relevant targets from the coordinated nitric oxide of DNICs.

The intriguing chemical reactivity and potential biological functions open avenues to explore the uncharted territory of DNICs associated with molecular catalysts and pharmaceutical applications. The flexibility and hemilability of coordination numbers among four-, five-, and six-coordinate DNICs promising binding and releasing of substrates, reversible interconversion of $\{\text{Fe}(\text{NO})_2\}^9/^{10}$ DNICs, and transient reduction species of $\{\text{Fe}(\text{NO})_2\}^{10}$ DNICs serving as electron reservoir for the delivery and uptake of electrons and the incorporation of proton relay from chelating coordinate ligands of DNICs initiating the subsequent substrate activation rationalize the uniqueness of DNICs acting as efficient molecular catalysts. Also, the controlled nitrosylation of critical biological targets by coordinated NO of DNICs modulating the physiological responses via selectively triggering NO-dependent signaling pathways may be employed for pharmaceutical applications. Inspired by the unambiguous assignments of the Fe and NO oxidation states as $\{\text{Fe}^{\text{III}}(\text{NO}^-)_2\}^9$, DNICs as storage and transport agents of stable inorganic NO⁻/HNO donors for treating acute cardiac arrest in patients with congestive heart failure could be a promising direction for the future design of cardiac medicine.³ The continuous journey from the fundamental understandings of DNICs to their applications as molecular catalysts or pharmaceutical drugs hopefully sheds light on the prospects for human health in the future.

■ AUTHOR INFORMATION

Corresponding Author

*E-mail: wliaw@mx.nthu.edu.tw.

Funding

We gratefully acknowledge financial support from the Ministry of Science and Technology (Taiwan).

Notes

The authors declare no competing financial interest.

Biographies

Ming-Li Tsai received his B.S. in chemistry from National Central University in 2002 and obtained his M.S. and Ph.D. degrees under the supervision of Prof. Wen-Feng Liaw at National Tsing Hua University in 2004 and 2008. He carried out postdoctoral research under Prof. Edward I. Solomon at Stanford University in 2010–2013. He is now a research associate at National Tsing Hua University.

Chih-Chin Tsou received his B.S., M.S., and Ph.D. degrees in chemistry from National Tsing Hua University in 2005, 2007, and 2012 under the supervision of Prof. Wen-Feng Liaw. He is currently a research associate under the supervision Prof. James M. Mayer at Yale University.

Wen-Feng Liaw is distinguished Professor at National Tsing Hua University. He received his bachelor degree in chemistry from National Chung Hsing University in 1981 and Ph.D. degree from Texas A&M University in 1989. His research interests focus on biomimetic synthesis, inorganic spectroscopy, and biological applications, in particular, molecular catalysts for water splitting generating hydrogen and small molecule (NO_2^- , NO_3^-) activation by bioinspired dinitrosyl iron complexes (DNICs), as well as seeking new $\text{NO}/\text{H}_2\text{S}$ donor vehicles (DNICs and RREs) capable of delivering precise NO to specific targets.

■ REFERENCES

- (1) Murad, F. Discovery of Some of the Biological Effects of Nitric Oxide and Its Role in Cell Signaling (Nobel Lecture). *Angew. Chem., Int. Ed.* **1999**, *38*, 1856–1868.
- (2) Choi, Y.-B.; Tennesi, L.; Le, D. A.; Ortiz, J.; Bai, G.; Chen, H.-S. V.; Lipton, S. A. Molecular Basis of NMDA Receptor-Coupled Ion Channel Modulation by S-Nitrosylation. *Nat. Neurosci.* **2000**, *3*, 15–21.
- (3) Ignarro, L. J. Nitric Oxide: A Unique Endogenous Signaling Molecule in Vascular Biology (Nobel Lecture). *Angew. Chem., Int. Ed.* **1999**, *38*, 1882–1892.
- (4) Miranda, K. M. The Chemistry of Nitroxyl (HNO) and Implications in Biology. *Coord. Chem. Rev.* **2005**, *249*, 433–455.
- (5) Butler, A. R.; Megson, I. L. Non-Heme Iron Nitrosyls in Biology. *Chem. Rev.* **2002**, *102*, 1155–1166.
- (6) Hayton, T. W.; Legzdins, P.; Sharp, W. B. Coordination and Organometallic Chemistry of Metal–NO Complexes. *Chem. Rev.* **2002**, *102*, 935–992.
- (7) McDonald, C. C.; Phillips, W. D.; Mower, H. F. An Electron Spin Resonance Study of Some Complexes of Iron, Nitric Oxide, and Anionic Ligands. *J. Am. Chem. Soc.* **1965**, *87*, 3319–3326.
- (8) Vanin, A. F. Endothelium-Derived Relaxing Factor Is a Nitrosyl Iron Complex with Thiol Ligands. *FEBS Lett.* **1991**, *289*, 1–3.
- (9) Enemark, J. H.; Feltham, R. D. Principles of Structure, Bonding, and Reactivity for Metal Nitrosyl Complexes. *Coord. Chem. Rev.* **1974**, *13*, 339–406.
- (10) Hung, M.-C.; Tsai, M.-C.; Lee, G.-H.; Liaw, W.-F. Transformation and Structural Discrimination between the Neutral $\{\text{Fe}(\text{NO})_2\}^{10}$ Dinitrosyliron Complexes (DNICs) and the Anionic/Cationic $\{\text{Fe}(\text{NO})_2\}^9$ DNICs. *Inorg. Chem.* **2006**, *45*, 6041–6047.
- (11) Tsai, M.-L.; Hsieh, C.-H.; Liaw, W.-F. Dinitrosyl Iron Complexes (DNICs) Containing S/N/O Ligation: Transformation of Roussin's Red Ester into the Neutral $\{\text{Fe}(\text{NO})_2\}^{10}$ DNICs. *Inorg. Chem.* **2007**, *46*, 5110–5117.
- (12) Tsou, C.-C.; Lu, T.-T.; Liaw, W.-F. EPR, UV–Vis, IR, and X-ray Demonstration of the Anionic Dimeric Dinitrosyl Iron Complex $[(\text{NO})_2\text{Fe}(\mu\text{-S}^t\text{Bu})_2\text{Fe}(\text{NO})_2]^-$: Relevance to the Products of Nitrosylation of Cytosolic and Mitochondrial Aconitases, and High-Potential Iron Proteins. *J. Am. Chem. Soc.* **2007**, *129*, 12626–12627.
- (13) Chen, Y.-J.; Ku, W.-C.; Feng, L.-T.; Tsai, M.-L.; Hsieh, C.-H.; Hsu, W.-H.; Liaw, W.-F.; Hung, C.-H.; Chen, Y.-J. Nitric Oxide Physiological Responses and Delivery Mechanisms Probed by Water-Soluble Roussin's Red Ester and $\{\text{Fe}(\text{NO})_2\}^{10}$ DNIC. *J. Am. Chem. Soc.* **2008**, *130*, 10929–10938.
- (14) Tsai, F.-T.; Kuo, T.-S.; Liaw, W.-F. Dinitrosyl Iron Complexes (DNICs) Bearing O-Bound Nitrito Ligand: Reversible Transformation between the Six-Coordinate $\{\text{Fe}(\text{NO})_2\}^9$ $[(1\text{-MeIm})_2(\eta^2\text{-ONO})\text{Fe}(\text{NO})_2]$ ($g = 2.013$) and Four-Coordinate $\{\text{Fe}(\text{NO})_2\}^9$ $[(1\text{-MeIm})(\text{ONO})\text{Fe}(\text{NO})_2]$ ($g = 2.03$). *J. Am. Chem. Soc.* **2009**, *131*, 3426–3427.
- (15) Tsai, M.-C.; Tsai, F.-T.; Lu, T.-T.; Tsai, M.-L.; Wei, Y.-C.; Hsu, I. J.; Lee, J.-F.; Liaw, W.-F. Relative Binding Affinity of Thiolate, Imidazolate, Phenoxide, and Nitrite Toward the $\{\text{Fe}(\text{NO})_2\}$ Motif of Dinitrosyl Iron Complexes (DNICs): The Characteristic Pre-Edge Energy of $\{\text{Fe}(\text{NO})_2\}^9$ DNICs. *Inorg. Chem.* **2009**, *48*, 9579–9591.
- (16) Lu, T.-T.; Chen, C.-H.; Liaw, W.-F. Formation of the Distinct Redox-Interrelated Forms of Nitric Oxide from Reaction of Dinitrosyl Iron Complexes (DNICs) and Substitution Ligands. *Chem.—Eur. J.* **2010**, *16*, 8088–8095.
- (17) Tsai, F.-T.; Chen, P.-L.; Liaw, W.-F. Roles of the Distinct Electronic Structures of the $\{\text{Fe}(\text{NO})_2\}^9$ and $\{\text{Fe}(\text{NO})_2\}^{10}$ Dinitrosyliron Complexes in Modulating Nitrite Binding Modes and Nitrite Activation Pathways. *J. Am. Chem. Soc.* **2010**, *132*, 5290–5299.
- (18) Tsou, C.-C.; Liaw, W.-F. Transformation of the $\{\text{Fe}(\text{NO})_2\}^9$ Dinitrosyl Iron Complexes (DNICs) into S-Nitrosothiols (RSNOs) Triggered by Acid–Base Pairs. *Chem.—Eur. J.* **2011**, *17*, 13358–13366.
- (19) Shih, W. C.; Lu, T. T.; Yang, L. B.; Tsai, F. T.; Chiang, M. H.; Lee, J. F.; Chiang, Y. W.; Liaw, W. F. New Members of a Class of Dinitrosyliron Complexes (DNICs): The Characteristic EPR Signal of the Six-Coordinate and Five-Coordinate $\{\text{Fe}(\text{NO})_2\}^9$ DNICs. *J. Inorg. Biochem.* **2012**, *113*, 83–93.
- (20) Tsai, F.-T.; Lee, Y.-C.; Chiang, M.-H.; Liaw, W.-F. Nitrate-to-Nitrite-to-Nitric Oxide Conversion Modulated by Nitrate-Containing $\{\text{Fe}(\text{NO})_2\}^9$ Dinitrosyl Iron Complex (DNIC). *Inorg. Chem.* **2013**, *52*, 464–473.
- (21) Yeh, S.-W.; Lin, C.-W.; Li, Y.-W.; Hsu, I. J.; Chen, C.-H.; Jang, L.-Y.; Lee, J.-F.; Liaw, W.-F. Insight into the Dinuclear $\{\text{Fe}(\text{NO})_2\}^{10}\{\text{Fe}(\text{NO})_2\}^{10}$ and Mononuclear $\{\text{Fe}(\text{NO})_2\}^{10}$ Dinitrosyliron Complexes. *Inorg. Chem.* **2012**, *51*, 4076–4087.
- (22) Tsou, C.-C.; Chiu, W.-C.; Ke, C.-H.; Tsai, J.-C.; Wang, Y.-M.; Chiang, M.-H.; Liaw, W.-F. Iron(III) Bound by Hydrosulfide Anion Ligands: NO-Promoted Stabilization of the $[\text{Fe}^{\text{III}}\text{-SH}]$ Motif. *J. Am. Chem. Soc.* **2014**, *136*, 9424–9433.
- (23) Yeh, S.-W.; Tsou, C.-C.; Liaw, W.-F. The Dinitrosyliron Complex $[\text{Fe}_4(\mu_3\text{-S})_2(\mu_2\text{-NO})_2(\text{NO})_6]^{2-}$ Containing Bridging Nitroxyls: ^{15}N (NO) NMR Analysis of the Bridging and Terminal NO-Coordinate Ligands. *Dalton Trans.* **2014**, *43*, 9022–9025.
- (24) Reginato, N.; McCrory, C. T. C.; Pervitsky, D.; Li, L. Synthesis, X-ray Crystal Structure, and Solution Behavior of $\text{Fe}(\text{NO})_2(1\text{-MeIm})_2$: Implications for Nitrosyl Non-Heme-Iron Complexes with $g = 2.03$. *J. Am. Chem. Soc.* **1999**, *121*, 10217–10218.
- (25) Tsou, C.-C.; Yang, W.-L.; Liaw, W.-F. Nitrite Activation to Nitric Oxide via One-fold Protonation of Iron(II)-O,O-nitrito Complex: Relevance to the Nitrite Reductase Activity of Deoxyhemoglobin and Deoxyhemerythrin. *J. Am. Chem. Soc.* **2013**, *135*, 18758–18761.
- (26) Lin, Z.-S.; Chiou, T.-W.; Liu, K.-Y.; Hsieh, C.-C.; Yu, J.-S. K.; Liaw, W.-F. A Dinitrosyliron Complex within the Homoleptic

Fe(NO)₄ Anion: NO as Nitroxyl and Nitrosyl Ligands within a Single Structure. *Inorg. Chem.* **2012**, *51*, 10092–10094.

(27) Tsou, C.-C.; Tsai, F.-T.; Chen, H.-Y.; Hsu, I. J.; Liaw, W.-F. Insight into One-Electron Oxidation of the {Fe(NO)₂}⁹ Dinitrosyl Iron Complex (DNIC): Aminyl Radical Stabilized by [Fe(NO)₂] Motif. *Inorg. Chem.* **2013**, *52*, 1631–1639.

(28) Lin, Z.-S.; Lo, F.-C.; Li, C.-H.; Chen, C.-H.; Huang, W.-N.; Hsu, I. J.; Lee, J.-F.; Horng, J.-C.; Liaw, W.-F. Peptide-Bound Dinitrosyliron Complexes (DNICs) and Neutral/Reduced-Form Roussin's Red Esters (RREs/rRREs): Understanding Nitrosylation of [Fe–S] Clusters Leading to the Formation of DNICs and RREs Using a *De Novo* Design Strategy. *Inorg. Chem.* **2011**, *50*, 10417–10431.

(29) Grabarczyk, D. B.; Ash, P. A.; Vincent, K. A. Infrared Spectroscopy Provides Insight into the Role of Dioxygen in the Nitrosylation Pathway of a [2Fe2S] Cluster Iron–Sulfur Protein. *J. Am. Chem. Soc.* **2014**, *136*, 11236–11239.

(30) Lu, T.-T.; Lai, S.-H.; Li, Y.-W.; Hsu, I. J.; Jang, L.-Y.; Lee, J.-F.; Chen, I. C.; Liaw, W.-F. Discrimination of Mononuclear and Dinuclear Dinitrosyl Iron Complexes (DNICs) by S K-Edge X-ray Absorption Spectroscopy: Insight into the Electronic Structure and Reactivity of DNICs. *Inorg. Chem.* **2011**, *50*, 5396–5406.

(31) Ye, S.; Neese, F. The Unusual Electronic Structure of Dinitrosyl Iron Complexes. *J. Am. Chem. Soc.* **2010**, *132*, 3646–3647.

(32) Lancaster, K. M.; Roemelt, M.; Ettenhuber, P.; Hu, Y.; Ribbe, M. W.; Neese, F.; Bergmann, U.; DeBeer, S. X-ray Emission Spectroscopy Evidences a Central Carbon in the Nitrogenase Iron–Molybdenum Cofactor. *Science* **2011**, *334*, 974–977.

(33) Lu, T.-T.; Weng, T.-C.; Liaw, W.-F. X-Ray Emission Spectroscopy: A Spectroscopic Measure for the Determination of NO Oxidation States in Fe–NO Complexes. *Angew. Chem., Int. Ed.* **2014**, *53*, 11562–11566.

(34) Berto, T. C.; Speelman, A. L.; Zheng, S.; Lehnert, N. Mono- and dinuclear non-heme iron–nitrosyl complexes: Models for key intermediates in bacterial nitric oxide reductases. *Coord. Chem. Rev.* **2013**, *257*, 244–259.

(35) Tonzetich, Z. J.; Wang, H.; Mitra, D.; Tinberg, C. E.; Do, L. H.; Jenney, F. E.; Adams, M. W. W.; Cramer, S. P.; Lippard, S. J. Identification of Protein-Bound Dinitrosyl Iron Complexes by Nuclear Resonance Vibrational Spectroscopy. *J. Am. Chem. Soc.* **2010**, *132*, 6914–6916.

(36) Hess, J. L.; Hsieh, C.-H.; Brothers, S. M.; Hall, M. B.; Darenbourg, M. Y. Self-Assembly of Dinitrosyl Iron Units into Imidazolate-Edge-Bridged Molecular Squares: Characterization Including Mössbauer Spectroscopy. *J. Am. Chem. Soc.* **2011**, *133*, 20426–20434.

(37) Tinberg, C. E.; Tonzetich, Z. J.; Wang, H.; Do, L. H.; Yoda, Y.; Cramer, S. P.; Lippard, S. J. Characterization of Iron Dinitrosyl Species Formed in the Reaction of Nitric Oxide with a Biological Rieske Center. *J. Am. Chem. Soc.* **2010**, *132*, 18168–18176.

(38) Landry, A. P.; Duan, X.; Huang, H.; Ding, H. Iron-Sulfur Proteins are the Major Source of Protein-Bound Dinitrosyl Iron Complexes Formed in *Escherichia coli* Cells under Nitric Oxide Stress. *Free Radical Biol. Med.* **2011**, *50*, 1582–1590.

(39) Rogers, P. A.; Eide, L.; Klungland, A.; Ding, H. Reversible Inactivation of *E. coli* Endonuclease III via Modification of Its [4Fe-4S] Cluster by Nitric Oxide. *DNA Repair* **2003**, *2*, 809–817.

(40) Lo, F.-C.; Lee, J.-F.; Liaw, W.-F.; Hsu, I. J.; Tsai, Y.-F.; Chan, S. I.; Yu, S. S. F. The Metal Core Structures in the Recombinant *Escherichia coli* Transcriptional Factor SoxR. *Chem.—Eur. J.* **2012**, *18*, 2565–2577.

(41) Yang, W.; Rogers, P. A.; Ding, H. Repair of Nitric Oxide-Modified Ferredoxin [2Fe-2S] Cluster by Cysteine Desulfurase (IscS). *J. Biol. Chem.* **2002**, *277*, 12868–12873.

(42) Lu, T.-T.; Chiou, S.-J.; Chen, C.-Y.; Liaw, W.-F. Mononitrosyl Tris(Thiolate) Iron Complex [Fe(NO)(SPh)₃][−] and Dinitrosyl Iron Complex [(EtS)₂Fe(NO)₂][−]: Formation Pathway of Dinitrosyl Iron Complexes (DNICs) from Nitrosylation of Biomimetic Rubredoxin [Fe(SR)₄]^{2−/1−} (R = Ph, Et). *Inorg. Chem.* **2006**, *45*, 8799–8806.

(43) Lu, T.-T.; Huang, H.-W.; Liaw, W.-F. Anionic Mixed Thiolate–Sulfide-Bridged Roussin's Red Esters [(NO)₂Fe(μ-SR)(μ-S)Fe(NO)₂][−] (R = Et, Me, Ph): A Key Intermediate for Transformation of Dinitrosyl Iron Complexes (DNICs) to [2Fe-2S] Clusters. *Inorg. Chem.* **2009**, *48*, 9027–9035.

(44) Tsai, M.-L.; Chen, C.-C.; Hsu, I. J.; Ke, S.-C.; Hsieh, C.-H.; Chiang, K.-A.; Lee, G.-H.; Wang, Y.; Chen, J.-M.; Lee, J.-F.; Liaw, W.-F. Photochemistry of the Dinitrosyl Iron Complex [S₂Fe(NO)₂][−] Leading to Reversible Formation of [S₂Fe(μ-S)₂FeS₂]^{2−}: Spectroscopic Characterization of Species Relevant to the Nitric Oxide Modification and Repair of [2Fe–2S] Ferredoxins. *Inorg. Chem.* **2004**, *43*, 5159–5167.

(45) Tsou, C.-C.; Lin, Z.-S.; Lu, T.-T.; Liaw, W.-F. Transformation of Dinitrosyl Iron Complexes [(NO)₂Fe(SR)₂][−] (R = Et, Ph) into [4Fe-4S] Clusters [Fe₄S₄(SPh)₄]^{2−}: Relevance to the Repair of the Nitric Oxide-Modified Ferredoxin [4Fe-4S] Clusters. *J. Am. Chem. Soc.* **2008**, *130*, 17154–17160.

(46) Chazov, E. I.; Rodnenkov, O. V.; Zorin, A. V.; Lakomkin, V. L.; Gramovich, V. V.; Vyborov, O. N.; Dragnev, A. G.; Timoshin, C. A.; Buryachkovskaya, L. L.; Abramov, A. A.; Massenko, V. P.; Arzamastsev, E. V.; Kapelko, V. I.; Vanin, A. F. Hypotensive Effect of Oxacom Containing a Dinitrosyl Iron Complex with Glutathione: Animal Studies and Clinical Trials on Healthy Volunteers. *Nitric Oxide* **2012**, *26*, 148–156.

(47) Wen, Y.-D.; Ho, Y.-L.; Shiau, R.-J.; Yeh, J.-K.; Wu, J.-Y.; Wang, W.-L.; Chiou, S.-J. Synergistic Antitumor Effect of Curcumin and Dinitrosyl Iron Complexes for against Melanoma Cells. *J. Organomet. Chem.* **2010**, *695*, 352–359.

(48) Bosworth, C. A.; Toledo, J. C., Jr.; Zmijewski, J. W.; Li, Q.; Lancaster, J. R., Jr. Dinitrosyliron Complexes and the Mechanism(s) of Cellular Protein Nitrosothiol Formation from Nitric Oxide. *Proc. Natl. Acad. Sci. U. S. A.* **2009**, *106*, 4671–4676.

(49) Boese, M.; Keese, M. A.; Becker, K.; Busse, R.; Mulsch, A. Inhibition of Glutathione Reductase by Dinitrosyl-Iron-Dithiolate Complex. *J. Biol. Chem.* **1997**, *272*, 21767–21773.

(50) Lundberg, J. O.; Weitzberg, E.; Gladwin, M. T. The Nitrate–Nitrite–Nitric Oxide Pathway in Physiology and Therapeutics. *Nat. Rev. Drug Discovery* **2008**, *7*, 156–167.

(51) Wasser, I. M.; de Vries, S.; Moënné-Loccoz, P.; Schröder, I.; Karlin, K. D. Nitric Oxide in Biological Denitrification: Fe/Cu Metalloenzyme and Metal Complex NO_x Redox Chemistry. *Chem. Rev.* **2002**, *102*, 1201–1234.

(52) Reddy, D.; Lancaster, J. R., Jr.; Cornforth, D. P. Nitrite Inhibition of *Clostridium botulinum*: Electron Spin Resonance Detection of Iron-Nitric Oxide Complexes. *Science* **1983**, *221*, 769–770.

(53) Yi, J.; Heinecke, J.; Tan, H.; Ford, P. C.; Richter-Addo, G. B. The Distal Pocket Histidine Residue in Horse Heart Myoglobin Directs the O-Binding Mode of Nitrite to the Heme Iron. *J. Am. Chem. Soc.* **2009**, *131*, 18119–18128.

(54) Khin, C.; Heinecke, J.; Ford, P. C. Oxygen Atom Transfer from Nitrite Mediated by Fe(III) Porphyrins in Aqueous Solution. *J. Am. Chem. Soc.* **2008**, *130*, 13830–13831.

(55) Patra, A. K.; Afshar, R. K.; Rowland, J. M.; Olmstead, M. M.; Mascharak, P. K. Thermally Induced Stoichiometric and Catalytic O-Atom Transfer by a Non-Heme Iron(III)–Nitro Complex: First Example of Reversible {Fe–NO}⁷ ↔ Fe^{III}–NO₂ Transformation in the Presence of Dioxygen. *Angew. Chem., Int. Ed.* **2003**, *115*, 4655–4659.

(56) Miljkovic, J. L.; Kenkel, I.; Ivanovic-Burmazovic, I.; Filipovic, M. R. Generation of HNO and HSNO from Nitrite by Heme-Iron-Catalyzed Metabolism with H₂S. *Angew. Chem., Int. Ed.* **2013**, *52*, 12061–12064.

(57) Tran, C. T.; Williard, P. G.; Kim, E. Nitric Oxide Reactivity of [2Fe-2S] Clusters Leading to H₂S Generation. *J. Am. Chem. Soc.* **2014**, *136*, 11874–11877.